Stochastic channel simulator based on local scattering functions

Y. Isukapalli, H. C. Song, and W. S. Hodgkiss
Scripps Institution of Oceanography, University of California, San Diego, La Jolla, California 92093-0238
yogananda.isukapalli@gmail.com, hcsong@ucsd.edu, wsh@ucsd.edu

Abstract: This letter addresses the limitations of the stochastic channel simulation approach employed in wireless channels when directly applied to underwater channels. First it is shown analytically why the simulation method fails when the correlated taps each have a different Doppler spectrum. Then, based on the idea of local scattering functions, we propose a simple solution to the problem of simulating a channel with correlated taps where the correlated taps occur in subgroups with each of the subgroups having a different Doppler spectrum, applicable to underwater channels. Our simulation approach is tested successfully on the KAM08 channel.

PACS numbers: 43.60.Dh, 43.60.Cg [CG]
Date Received: June 8, 2011 **Date Accepted:** August 9, 2011

1. Introduction

Experimental evaluation of the effects of the underwater acoustic (UA) channel on the performance of communication systems often involves considerable effort, and these experiments are quite expensive to conduct. Reproducing a statistically consistent channel in simulation is of great interest to the underwater research community because it would significantly reduce the effort and cost associated with actually carrying out a field experiment.[1] The idea behind statistical channel generation is as follows. The UA channel is measured repeatedly over a period of time during an underwater experiment. Because multiple channel measurements are available, one can have a reasonably accurate statistical characterization of the UA channel. The generation of the channel (in simulation) is then carried out with an aim to mimic the statistical behavior of the measured channel. One can test various communication system design methods on the channel generated in simulation. If the simulated channel is statistically consistent with the measured channel, then one can be reasonably confident that the performance results obtained in simulation would be sufficiently close to the actual system performance at sea.

Statistical channel generation also has been of great interest to the wireless research community. A popular channel generation method employed in wireless channels has been presented in a detailed tutorial manner in Ref. 2. Recently, the method has been adapted successfully for an underwater acoustic channel.[3] As will be explained later, however, the method has some limitations. The channel generation method is applicable to channels when (1) the taps are uncorrelated with the same or different Doppler spectrum at each of the taps or (2) the taps are correlated with the same Doppler spectrum. Most of the wireless channels satisfy the uncorrelated taps assumption, and hence the wireless community has not paid much attention to the case of correlated taps with different Doppler spectra.

When the channel simulation methodology in Ref. 3 was applied to the channel measured during the KAM08 experiment,[4] it was difficult to achieve a good match between the scattering functions of the measured channel and the simulated channel. This is due to the fact that the KAM08 channel taps are correlated in subgroups with

the different subgroups having different Doppler spectra. To simulate the KAM08 channel, this letter will incorporate the concept of local scattering functions[5] where each local scattering function has either uncorrelated taps or correlated taps each with the same Doppler spectrum. Although this is a relatively simple extension of the method in Ref. 3, the results obtained turn out to be quite useful in terms of statistical consistency between the measured and simulated channels as illustrated in Sec. 4.

The basics of the channel simulator are described in Sec. 2. Section 3 explains analytically why the methodology in Ref. 2 fails when we have correlated channel taps with different Doppler spectra. In Sec. 4, simulation results are presented illustrating the effectiveness of the channel simulator based on local scattering functions.

Notation: Small and upper case bold letters indicate vector and matrix, respectively. $E(.)$, $(.)^T$, $(.)^H$, $|.|$, $(.)^*$, and $\|.\|$ denote expectation, transpose, Hermitian, absolute value, complex conjugate, and 2-norm, respectively. $x \sim p(x)$ indicates that the random variable x is distributed as $p(x)$. $\mathbf{x} \sim \mathcal{NC}(\boldsymbol{\mu}, \boldsymbol{\Sigma})$ indicates a circularly symmetric complex Gaussian (CSCG) random variable x with mean μ and covariance Σ. $\mathcal{F}\{f(x)\}$ denotes the Fourier transform of function $f(x)$.

2. System design

In this section, we review the basic concepts used in the channel simulator. Let the time-varying channel impulse response be $h(\tau, t)$. The variable τ indicates the delay, and t indicates the temporal variation of the channel. In a discrete-time model, τ would be discrete, and it indicates the tap number in the tapped-delay line channel structure. The channel autocorrelation function evaluated with respect to "t" at a fixed "τ" tap is given by

$$R_h(\tau, \Delta t) = E[h^*(\tau, t)h(\tau, t + \Delta t)]. \tag{1}$$

The scattering function $P(\tau, v)$ is obtained by taking the Fourier transform of the channel autocorrelation function $R_h(\tau, \Delta t)$. Note that the Fourier transform is taken with respect to the variable Δt,

$$P(\tau, \upsilon) = \mathcal{F}[R_h(\tau, \Delta t)]. \tag{2}$$

For a detailed tutorial presentation on scattering functions, the reader is referred to Refs. 2 and 3. We assume that there are M taps in the tapped-delay line structure of the channel. The statistically consistent reproduction of the scattering function requires the following two conditions:

(1) The autocorrelation function of the simulated channel and the measured channel match at each of the taps. Let $g_k(t)$, $k = \{1, \ldots, M\}$ be the stochastic/simulated channel, and $h_k(t)$, $k = \{1, \ldots, M\}$ be the measured channel. Then the preceding condition implies that

$$R_{gk}(\Delta t) = R_{hk}(\Delta t), \tag{3}$$

where $R_{gk}(\Delta t)$ is the autocorrelation function of $g(t)$ at the kth simulated tap and $R_{hk}(\Delta t)$ is the autocorrelation function of $h(t)$ at the kth measured tap. Note that if the autocorrelation functions match, the scattering functions also would match.

(2) The simulated tap cross-correlation matrix matches that of the tap cross-correlation matrix obtained from the measured channel impulse responses (CIRs). By stacking the channel taps in vector form, we can write the stochastic/simulated channel vector as $\mathbf{g} = [g_1, g_2, \ldots, g_M]^T$ and the measured channel vector as $\mathbf{h} = [h_1, h_2, \ldots, h_M]^T$ (for simplicity time variable t is dropped). Then, the preceding condition implies that

$$E\left[\mathbf{h}\mathbf{h}^H\right] = E\left[\mathbf{g}\mathbf{g}^H\right] = \mathbf{R}. \tag{4}$$

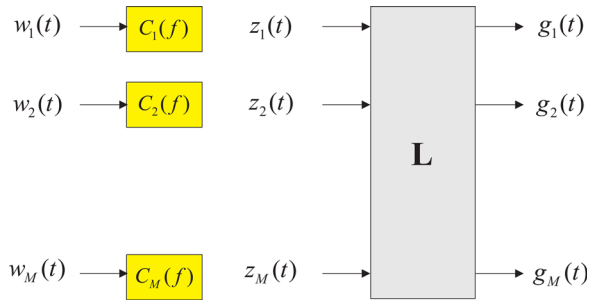

Fig. 1. (Color online) Stochastic channel simulator block diagram. Independent bandlimited white Gaussian noise sequences $w_k(t)$ are shaped by independent Doppler spectra $C_k(f)$ to generate a time-series $z_k(t)$ at each tap, and converted into tap gains $g_k(t)$ via the linear transformation L.

3. Stochastic channel simulator

Although it is pointed out in Ref. 2 that the simulation approach described is only valid for (1) uncorrelated taps or (2) correlated taps each with the same Doppler spectrum, there is no analytical explanation. In this section, this limitation is discussed in detail with explanation.

As per the method suggested in Ref. 2, the channel is simulated in two steps as illustrated in Fig. 1. The first step introduces the autocorrelation at each of the taps, and the cross-correlation of the taps is implemented in the second step. Introducing the temporal autocorrelation at each tap is equivalent to passing a bandlimited white noise process $w(t)$ (with flat spectrum in the frequency domain) through a spectrum shaping filter $C_k(f)$. The power spectral density at the output of the spectrum shaping filter (of the channel simulator) should be $\mathcal{F}\{R_{hk}(\Delta t)\}$.

The cross-correlation between the taps is achieved by making use of the Cholesky decomposition of the measured channel tap cross-correlation matrix $\mathbf{R}$ defined in Eq. (4). The Cholesky decomposition of $\mathbf{R}$ is given by

$$\mathbf{T}\mathbf{T}^H = \mathbf{R}. \tag{5}$$

Let the bandlimited white Gaussian noise input vector to the simulator be denoted as $\mathbf{w} = [w_1(t), w_2(t), \ldots, w_M(t)]^T$, $\mathbf{w} \sim \mathcal{NC}(0, \mathbf{I})$. The output vector after spectral shaping filters is denoted as $\mathbf{z} = [z_1(t), z_2(t), \ldots, z_M(t)]^T$. Because the elements of $\mathbf{w}$ are independent from each other, the correlation matrix of $\mathbf{z}$ will be a diagonal matrix,

$$\mathbf{D} = E\left[\mathbf{z}\mathbf{z}^H\right]. \tag{6}$$

The spectral shaped data vector $\mathbf{z}$ is then converted by $\mathbf{L}$ yielding the final simulated channel output vector $\mathbf{g} = [g_1(t), g_2(t), \ldots, g_M(t)]^T$,

$$\mathbf{g} = \mathbf{L}\mathbf{z}. \tag{7}$$

As will be explained later, to make sure that the simulated channel's correlation matrix and measured channel's correlation matrix match, $\mathbf{L}$ is chosen to be

$$\mathbf{L} = \mathbf{T}\mathbf{D}^{-1/2}. \tag{8}$$

Note that $\mathbf{D}$ is a full rank diagonal matrix hence construction of $\mathbf{D}^{-1/2}$ is not a problem. It is easy to verify that the simulated tap cross-correlation matrix matches the measured tap cross-correlation matrix as follows:

$$\begin{aligned} E\left(\mathbf{g}\mathbf{g}^H\right) &= E\left[(\mathbf{L}\mathbf{z})(\mathbf{L}\mathbf{z})^H\right] = E\left[\left(\mathbf{L}\mathbf{z}\mathbf{z}^H\mathbf{L}^H\right)\right] = \mathbf{L}\left[E\left(\mathbf{z}\mathbf{z}^H\right)\right]\mathbf{L}^H \\ &= \mathbf{T}\mathbf{D}^{-1/2}\left[E\left(\mathbf{z}\mathbf{z}^H\right)\right]\mathbf{D}^{-1/2}\mathbf{T}^H = \mathbf{T}\mathbf{T}^H = \mathbf{R}. \end{aligned} \tag{9}$$

In the preceding formulation, if all of the taps have the same Doppler spectrum, then we have $\mathbf{D} = \mathbf{I}$ and $\mathbf{L} = \mathbf{T}$.

Let us take a closer look at the power spectral density of the kth tap of the channel simulator output $g_k(t)$,

$$g_k(t) = l_{k1}z_1(t) + l_{k2}z_2(t) + \cdots + l_{kk}z_k(t),$$

where $[l_{k1}, l_{k2}, \ldots, l_{kk}]$ is the kth row of $\mathbf{L}$. The autocorrelation of $g_k(t)$ is given by

$$R_{gk}(\Delta t) = E\left[g_k^*(t)g_k(t+\Delta t)\right]. \tag{10}$$

Because z_k and z_l are independent random processes (for all $k \neq l$), the autocorrelation of $g_k(t)$ simplifies to

$$R_{gk}(\Delta t) = |l_{k1}|^2 R_{z1}(\Delta t) + |l_{k2}|^2 R_{z2}(\Delta t) + \cdots + |l_{kk}|^2 R_{zk}(\Delta t). \tag{11}$$

To reproduce accurately a statistically consistent channel, however, the autocorrelation of $g_k(t)$ at each tap (and subsequently the power spectral density) should match the autocorrelation of $z_k(t)$ at each tap. From Eq. (11), a match in the autocorrelation can be achieved if and only if

(1) The taps are un-correlated, implying that $l_{ki} = 0$ if $k \neq i$.
(2) All the taps have the same autocorrelation, implying that $R_{zi} = R_{zk}$ for all i and k.

The popular channel simulation approach suggested in Ref. 2, and adopted for measured underwater channels in Ref. 3, thus is limited to scenarios where (1) the taps are uncorrelated or (2) all of the taps have the same power spectral density. In this paper, we analyze measured channel data collected during the KAM08 experiment.[4] It is found that the KAM08 channel does not satisfy either of the two conditions mentioned in the preceding, i.e., the taps of the measured KAM08 channel have noticeable cross-correlation as well as the power spectral density at each of the taps is not the same [see Fig. 2(b)].

To simulate channels similar to the channels observed during KAM08, we propose a simple yet effective channel simulation approach based on local scattering functions.[5] It should be mentioned that the idea of local scattering functions is more general than our usage of the term. In our local scattering function approach, the M taps are divided into P subgroups, $\{GR_1, GR_2, \ldots, GR_P\}$, wherein the taps in each of the subgroups are allowed to have cross-correlation but are not correlated with taps in another subgroup. Note that the number of taps in these subgroups need not be the same. The channel simulator now operates, in parallel, on each of the subgroups (subsequently on the corresponding local scattering function). Two main drawbacks of this approach are as follows: (1) one has to find a way to separate the scattering function into a number of smaller local scattering functions and (2) the computational complexity is now slightly higher due to the task of finding the Cholesky decomposition of the cross-correlation matrix in each subgroup. As shown in Sec. 4, this approach is found effective on the KAM08 channel data. It is conceivable, however, that the scattering function cannot easily be split into multiple local scattering functions.

4. Simulation results

In this section, we present simulation results showing the effectiveness of the local scattering function approach for the case of subgroups of channel taps having correlation with different subgroups each having a different Doppler spectrum. We begin with a brief description of the KAM08 experiment.[4]

The KAM08 experiment was carried out in shallow water off the western side of Kauai, Hawaii, over the period of June 16 to July 2, 2008. The objective of KMA08 was to collect acoustic and environmental data appropriate to study the

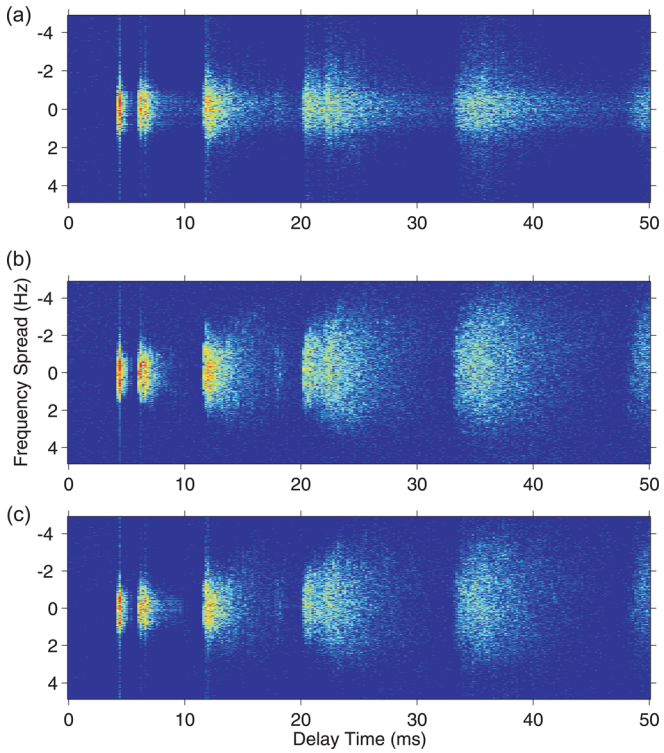

Fig. 2. (Color online) Scattering functions: (a) simulation based on the global scattering function, (b) data from KAM08, and (c) simulation based on local scattering functions. A noticeable difference between (a) and (b) is observed especially for the later group of arrivals in the context of Doppler spread and tails in delay spread, while (c) shows an improved resemblance to data (b). The dynamic range is 40 dB.

coupling of oceanography, acoustics, and underwater communications. Specifically we were interested in the impact of a fluctuating ocean environment and source/receiver motion on fluctuations in the acoustic channel impulse responses. The data analyzed in this letter are a transmission from a source towed by R/V Melville at 3 knots and at 50-m depth to a single element of a 16-element vertical array (Ch 11 at 76.5 m) moored at about 1.5 km range. The primary waveforms for channel probing were 30-s long, 511-digit m-sequences with a carrier frequency of 15 kHz and a chip rate of 5 kHz. Because we are dealing with a moving source, the broadband data is resampled with a mean Doppler shift to compensate for the motion.

The scattering function of the KAM08 data is shown in Fig. 2(b), indicating six noticeable groups of channel taps. Based on a ray model, the first and second arrivals correspond to direct and bottom-bounce paths, respectively. On the other hand, the subsequent arrivals interact with the dynamic sea surface, exhibiting a much broader micro-multipath structure in time (τ) along with a larger Doppler spread (v) induced by temporal variations. The scattering function has 251 taps corresponding to 50 ms of delay spread. Clearly, the power spectral density at each tap is not the same. Although not shown, the correlation matrix $\mathbf{R}$ also is found to be non-diagonal (i.e., correlated taps) but will be treated approximately as block-diagonal within each subgroup of arrivals.

The simulated scattering function in Fig. 2(a) is obtained in two steps as described in Sec. 3 (see Fig. 1). In the first step, the autocorrelation properties and in the second step the cross-correlation properties of the channel taps are satisfied. White noise $\mathbf{w}$ is passed through M (251) filters, where each filter has the corresponding Doppler spectrum shape and the resulting output $\mathbf{z}$ then is multiplied by $\mathbf{L}$ to arrive at

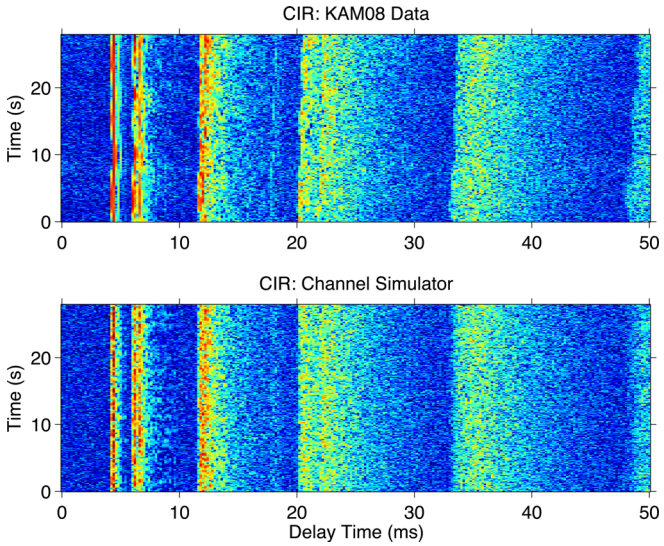

Fig. 3. (Color online) Channel impulse responses (CIRs) using the channel simulator (bottom) based on the local scattering function shown in Fig. 2(c) compared to the measured channel impulse responses from KAM08 data (top). The dynamic range is 40 dB.

the simulated channel $\mathbf{g}$. $\mathbf{L}$ is obtained from the Cholesky decomposition of the correlation matrix $\mathbf{R}$ (estimated with measured channel data). The resulting scattering function is shown in Fig. 2(a) calculated from $\mathbf{g}$ (note that $\mathbf{g}=\mathbf{L}\mathbf{z}$). Combining $\mathbf{z}$ with $\mathbf{L}$ (to arrive at $\mathbf{g}$) is done to preserve the channel tap correlation matrix. However, this comes at the cost of a distorted scattering function. As clearly illustrated in Figs. 2(a) and 2(b), the simulated/stochastic scattering function does not match the scattering function generated from the measured channel. A noticeable difference is observed especially for the later group of arrivals in the context of Doppler spread and tails in delay spread.

Because the measured scattering function shows that different subgroups of taps have different Doppler spectra, the simulation approach based on the complete (or global) scattering function does not work well as expected. Consequently, a simulation based on local scattering functions is applied as displayed in Fig. 2(c). Now the resemblance between the simulated Fig. 2(c) and measured Fig. 2(b) scattering functions is improved significantly as compared to Fig. 2(a). Finally, channel impulse responses (CIRs) are shown in Fig. 3 derived from the data (top) and simulator (bottom), suggesting that a channel simulator based on local scattering functions can generate CIRs which are statistically more consistent with the data.

References and links

[1]M. Siderius and M. B. Porter, "Modeling broadband ocean acoustic trans- missions with time-varying sea surfaces," J. Acoust. Soc. Am. **124**, 137–150 (2008).
[2]W. H. Tranter, K. S. Shanmugan, T. S. Rappaport, and K. L. Kosbar, in *Principles of Communication Systems Simulation with Wireless Applications* (Prentice Hall, Englewood Cliffs, NJ, 2004), Chap. 14.
[3]P. van Walree, T. Jenserud, and M. Smedsrud, "A discrete-time channel simulator driven by measured scattering functions," IEEE J. Select. Areas Commun. **26**, 1628–1637 (2008).
[4]T. Kang, H. C. Song, W. S. Hodgkiss, and J. S. Kim, "Long-range multi-carrier acoustic communications based on iterative sparse channel estimation," J. Acoust. Soc. Am. **128**, EL372–EL377 (2010).
[5]G. Matz, "On non-WSSUS wireless fading channels," IEEE Trans. Wireless Commun. **4**, 2465–2478 (2005).